J. Appl. Comput. Mech., 6(1) (2020) 13-25
DOI: 10.22055/JACM.2019.27482.1407

ISSN: 2383-4536
jacm.scu.ac.ir

M&MoCS

Shahid Chamran
University of Ahvaz

Journal of
Applied and Computational Mechanics

Research Paper

Sequential Implicit Numerical Scheme for Pollutant and Heat Transport in a Plane-Poiseuille Flow

Chinedu Nwaigwe

Department of Mathematics, Rivers State University, Port Harcourt, Nigeria

Received October 30 2018; Revised April 12 2019; Accepted for publication April 13 2019.
Corresponding author: Chinedu Nwaigwe (Nwaigwe.chinedu@ust.edu.ng)

Abstract. A sequential implicit numerical scheme is proposed for a system of partial differential equations defining the transport of heat and mass in the channel flow of a variable-viscosity fluid. By adopting the backward difference scheme for time derivative and the central difference scheme for the spatial derivatives, an implicit finite difference scheme is formulated. The variable-coefficient diffusive term in each equation is first expanded by differentiation. The next step of the sequential approach consists of providing a solution of the temperature and concentration, before providing a solution for the velocity. To verify the numerical scheme, the results are compared with those of a Matlab solver and a good agreement are found. We further conduct a numerical convergence analysis and found that the method is convergent. The numerical results are investigated against the model equations by studying the time evolution of the flow fields and found that the data, such as the boundary conditions, are perfectly verified. We then study the effects of the flow parameters on the flow fields. The results show that the Solutal and thermal Grashof numbers, as well as the pressure gradient parameter, increase the flow, while the Prandtl number and the pollutant injection parameter both decrease the flow. The conclusion of the study is that the sequential scheme has high numerical accuracy and convergent, while a change in the pollutant concentration leads to a small change in the flow velocity due to the opposing effects of viscosity and momentum source.

Keywords: Finite difference methods, Fluid flows, Sequential implicit method, Pollutant dispersion, Experimental order of convergence.

1. Introduction

The study of mass and heat diffusion in fluids is of considerable importance owing to many applications, like in molecular evaporators, rocket boosters, film vaporization in combustion chambers and cooling of re-entry vehicles [1]. In particular, it is paramount to monitor and possibly control the pollution of water bodies, for example, due to human activities [2]. In addition, understanding the heat distribution is important; an example of application is in the heating and cooling of the plate of a water bath [3]. Many industrial applications, such as heat exchangers, chemical distilleries and thermal protection systems, involve the combined influence of heat and mass transfer [4].

Consequently, a lot of researches have been devoted to this area. Umavathi and co-workers [5] analyzed the coupled effects of heat and mass transfer in a channel flow, incorporating the electrical conductivity and first order chemical reaction. They found that the thermal Grashof number, solutal Grashof number and the Brinkman number all increase the flow, while the parameters representing the chemical reaction and Hartman number decrease the flow. In [6], the effect of heat and mass transfer on the flow of an incompressible, constant viscosity, Newtonian fluid has been investigated. The model was analyzed using the finite element methods. Mebine, [7] also studied the thermal effects on a magneto-hydrodynamic pressure-driven flow. This author and co-workers [8, 9, 10] have investigated the effects of

Published online: July 05 2019

several conditions and parameters on flows through porous media including heat transfer in the soil. The MHD oscillatory flow of a Jeffrey fluid in a vertical porous channel with viscous dissipation have been investigated in [11], while the unsteady flow of a third grade fluid with combined heat and mass transfer in the presence of a chemical reaction is considered in [12].

In another study, the influence of heat transfers on electrically conducting Jeffrey fluid in a channel was studied in [13]. Murhuraj and co-workers [14] investigated the effects of thermal-diffusion, diffusion-thermo and space porosity on an MHD mixed convection flow of a micro-polar fluid; while the unsteady hydro-magnetic heat and mass transfer in natural convection flow past an exponentially accelerated vertical plate with hall current and rotation in the presence of thermal and mass diffusions was investigated in [15]. Also, the vertical channel flow of an electrically conducting fluid in the presence of Robin boundary condition was considered in [16].

Recently, the influence of chemical reaction and heat source on dissipative MHD mixed convection flow of a Casson nanofluid over a nonlinear permeable stretching sheet has been studied in [17]. Most of the investigations outlined above considered only constant properties such as constant viscosity and constant pollutant diffusion coefficients. Since many fluids can have variable viscosity, hence the attention of researchers have also been focused on the study of heat and mass transfer in the flow of variable viscosity fluids, see for example [18, 2, 3, 19]. Another study [4] considered the combined effects of heat and mass transfer on the flow of a temperature-dependent viscosity fluid. It is also shown that the velocity increases with increasing solutal and thermal Grashof numbers; while temperature-dependent thermal conductivity was considered for the fluid flow and heat transfer in nanofluid-filled channel in [20]. In the cases of variable-viscosity fluids or concentration-dependent mass diffusivity, the governing equations are nonlinear, hence closed form analytical solutions may not be possible. Therefore, numerical approaches have become very important tools.

In this paper, we extend the studies of Makinde and Chinyoka [2, 21, 3] by investigating the combined effects of heat and mass transfer on a fully developed flow of a concentration-dependent-viscosity fluid in a rectangular channel whose walls are controlled at a nonzero-constant temperature; we propose an implicit finite difference scheme that is implemented in a sequential manner. The resulting linear systems are diagonally dominant, so can be solved with fast and simple iterative linear solvers like the Gauss-Seidel algorithm. We conduct an experimental order of convergence to investigate the convergence of the method. Our results show that the method is convergent and computes the correct flow fields in line with the literature.

This paper is organized as follows; in section 2, the governing equations including the non-dimensional form are presented, while the sequential numerical algorithm is detailed in section 3. In section 4.1, a convergence analysis to demonstrate that the proposed numerical scheme is convergent is discussed; in section 4.2, the numerical scheme against a Matlab solver is validated; while in section 4.3, the computed solutions against the model is validated by verifying that the boundary conditions are satisfied. The effects of the flow parameters on the flow fields are presented and discussed in section 4.4. The paper ends in section 5 where the conclusions are made from the study.

2. Mathematical Formulation

Let $\Omega_c = \{(\bar{x},\bar{y},\bar{z}) : -a \le \bar{x} \le a, \bar{x},\bar{z} \in \Re\} \subset \Re^3$ be a channel whose walls are two stationary, parallel, infinitely large plates. Let the $\bar{x}$ - axis, which is along the channel axis, be vertically upward, the $\bar{y}$ -axis perpendicular to $\bar{x}$ -axis and the $\bar{z}$ -axis be perpendicular to $\overline{xy}$ - plane (see Fig. 1).

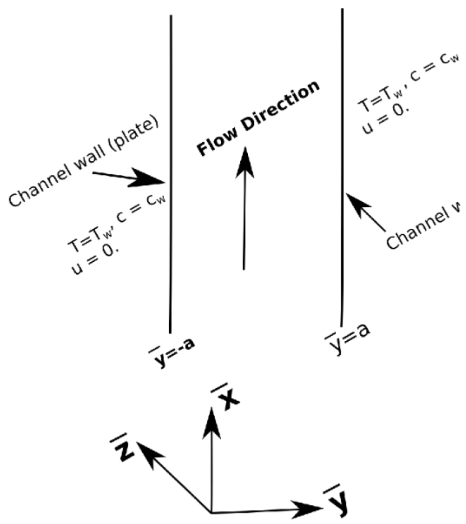

Fig. 1. Physical model of the flow of fluid, heat and pollutant in a channel

Consider the flow of an incompressible fluid with constant density, ρ in Ω_c . Suppose there is an injection of a pollutant into the fluid and that the fluid viscosity and the pollutant mass diffusivity are both concentration-dependent. Further assume a constant heating of the channel walls and that the flow is fully developed. The influences of the pollutant concentration and the temperature on the fluid flow is described following the Boussinesq approximation [2, 21, 4, 22]. The flow is unidirectional along the $\bar{x}$ axis so that the only non-zero velocity component is along the $\bar{x}$ direction. Since the flow is fully developed, the flow variations are only along the $\bar{y}$-axis. That is, the fluid velocity vector is given as $(u(\bar{y},\bar{t}), 0, 0)$. Therefore, the only non-vanishing spatial derivative is with respect to $\bar{y}$ (see Fig. 1). Consequently, all the convective terms vanish and the problem is governed by the following transport equations [2, 22, 21, 23, 24, 25]:

$$\frac{\partial u}{\partial \bar{t}} = -\frac{\partial p}{\partial \bar{x}} + \frac{\partial}{\partial \bar{y}}\left(\bar{\mu}(c)\frac{\partial u}{\partial \bar{y}}\right) + \rho\beta_c(c-c_0) + \rho\beta_T(T-T_0), \tag{1}$$

$$\frac{\partial C}{\partial \bar{t}} = \frac{\partial}{\partial \bar{y}}\left(\bar{D}(C)\frac{\partial C}{\partial \bar{y}}\right) + s(C), \tag{2}$$

$$\frac{\partial T}{\partial \bar{t}} = \alpha_T\frac{\partial^2 T}{\partial \bar{y}^2}, \quad -a<y<a,\ t>0, \tag{3}$$

$$\bar{\mu}(c) = \mu_0 e^{b_1(c-c_0)},\ \bar{D}(c) = De^{b_2(c-c_0)},\ S(c) = Qe^{b_3(c-c_0)}. \tag{4}$$

The above system is completed with the following initial and boundary conditions,

$$u(\bar{y},0) = m\left(1-\frac{\bar{y}^2}{a^2}\right),\ c(\bar{y},0) = c_0,\ T(\bar{y},0) = T_{0,}\ \ \bar{y}\in[-a,a], \tag{5}$$

$$\frac{\partial}{\partial \bar{y}}u(0,\bar{t}) = \frac{\partial}{\partial \bar{y}}c(0,\bar{t}) = \frac{\partial}{\partial \bar{y}}T(0,\bar{t}) = 0, \quad \bar{t}\geq 0, \tag{6}$$

$$u(a,\bar{t}) = 0,\ \ c(a,\bar{t}) = c_w,\ T(a,\bar{t}) = T_w,\ \ \bar{t}\geq 0, \tag{7}$$

where $\bar{t}$ is the time variable, $u(\bar{y},\bar{t})$, $c(\bar{y},\bar{t})$ and $T(\bar{y},\bar{t})$ are, respectively, the fluid velocity component along the $\bar{x}$ direction, the pollutant concentration and fluid temperature at point $\bar{y}$ at time $\bar{t}$. The quantities, P, ρ, g, β_c, β_T and α_T are the fluid pressure, density, the acceleration due to gravity, concentration expansion coefficient, temperature expansion coefficient and thermal conductivity respectively. The functions, $\bar{\mu}(c)$, $\bar{D}(c)$ and $S(c)$ model the fluid variable viscosity, the pollutant mass diffusion and the injection of the pollutant into the channel [2]. Also, T_w and c_w are the constant temperature and pollutant concentration at the channel walls (plates), a is half of the channel width, m is a real constant, while b_1, b_2, b_3, μ_0, D_0 and Q are, respectively, the viscosity variation parameter, pollutant diffusion variation parameter, external source variation parameter, fluid viscosity coefficient, pollutant diffusivity coefficient, and external source coefficient [2].

2.1. Non-Dimensionalization

To reduce the number of parameters appearing in the model and also eliminate the dimensionality of the variables and parameters of the model, the following dimensionless variables and parameters are introduced [25, 2]:

$$\begin{gathered} w = \frac{au}{\nu},\ f = \frac{c-c_0}{c_w-c_0},\ \theta = \frac{T-T_0}{T_a-T_0}, G_c = g\beta_c a^3\frac{c_w-c_0}{\nu^2},\ G_T = g\beta_T a^3\frac{T_w-T_0}{\nu^2}, \\ P_r = \frac{\nu}{\alpha_T},\ y = \frac{\bar{y}}{a}, x = \frac{\bar{x}}{a}, t = \frac{\nu}{a^2}, D = \frac{\bar{D}}{D_0},\ \mu = \frac{\bar{\mu}}{\mu_0},\ P = \frac{a^2\bar{P}}{\nu^2\rho},\ \nu = \frac{\mu_0}{\rho}, \\ K = -\frac{\partial P}{\partial x}, \alpha_T = b_1(c_w-c_0),\ \gamma = b_2(c_w-c_0),\ n = b_3(c_w-c_0),\ \lambda = \frac{Qa^2}{\nu(c_w-c_0)},\ S_c = \frac{\nu}{D_0}. \end{gathered} \tag{8}$$

Substituting the non-dimensional parameters in equation (8) into equations (1) - (7), the following non-dimensional equations are obtained:

$$\frac{\partial w}{\partial t} = K + \frac{\partial}{\partial \bar{y}}\left(e^{\alpha f}\frac{\partial w}{\partial y}\right) + G_c f + G_T\theta, \tag{9}$$

$$\frac{\partial f}{\partial t}=\frac{\partial}{\partial y}\left(e^{\gamma f}\frac{\partial f}{\partial y}\right)+\lambda e^{nf}, \tag{10}$$

$$\frac{\partial \theta}{\partial t}=\alpha_T\frac{\partial^2\theta}{\partial y^2},\quad 0<y<1,\, t>0, \tag{11}$$

subject to

$$w(y,0)=m(1-y^2),\ y\in[1,0],\ f(y,0)=\theta(y,0)=0,\, y\in[0,1). \tag{12}$$

$$\frac{\partial}{\partial y}w(0,t)=\frac{\partial}{\partial y}f(0,t)=\frac{\partial}{\partial y}\theta(0,t)=0,\ t\ge 0, \tag{13a}$$

$$w(1,t)=0,\ f(1,t)=\theta(1,t)=1,\ t\ge 0, \tag{13b}$$

where G_T, G_c, P_r, S_c and K are the thermal Grashof number, the solutal Grashof number, the Prandtl number, the Schmidt number and the pressure gradient respectively [25, 2].

3. Numerical Formulation

In this section, the method of solution for the system (9) to (13) are detailed and explored. Let M be a positive integer, define $h=1/M$ and let $\{y_i\}_{i=0}^{M}$ be a set of points that are within the domain $[0,1]$. Also, let $T\in\Re$ be a real number, and t_N is a discrete time such that $t_{N+1}=t_N+\Delta t$ with Δt given. We seek to find the following approximations:

$$w_i^N\approx w(y_i,t_N),\quad f_i^N\approx f(y_i,t_N),\ \theta_i^N\approx\theta(y_i,t_N). \tag{14}$$

In the following subsections, the numerical algorithms for each of the equations (9), (10) and (11) are formulated. The scheme is sequential such that equations (11) and (10) are first solved, then their results are used to compute w_i^{N+1} in (9). Backward difference scheme for time derivatives and central difference scheme for all spatial derivatives are considered. As a result, the following scheme is adopted for (11),

$$\theta_i^{N+1}=\theta_i^N+r^\theta(\theta_{i+1}^{N+1}-2\theta_i^{N+1}+\theta_{i-1}^{N+1}),\ \ for\ i=0,1,2,\ldots,M-1, \tag{15}$$

To solve equation (10), differentiation is first applied on the diffusion term [2], then the following implicit scheme is adopted:

$$f_i^{N+1}=f_i^N+r^f\left(f_{i+1}^{N+1}-2f_i^{N+1}+f_{i-1}^{N+1}+\frac{\gamma}{4}\left(f_{i+1}^N-f_{i-1}^N\right)\right)+\lambda e^{nf_i^N},\quad for\ i=0,1,2,\ldots,M-1, \tag{16}$$

where $r^f=\Delta t\, e^{\gamma f_i^N}r^\theta/(S_c(\Delta y)^2)=\Delta t/(P_r(\Delta y)^2)$. Similar to (16), we first expand the viscous term in (9), then adopt the following scheme:

$$\begin{aligned} w_i^{N+1}&=w_i^N+r^w(w_{i+1}^{N+1}-2w_i^{N+1}+w_{i-1}^{N+1})+\frac{\alpha}{4}r^w(f_{i+1}^{N+1}-f_{i-1}^{N+1})(w_{i+1}^N-w_{i-1}^N)\\ &+(G_cf_i^{N+1}+G_Tf_i^{N+1}+K)\Delta t,\quad 0\le i\le M-1,\end{aligned} \tag{17}$$

where $r^w=\Delta t\, e^{\alpha f_i^{N+1}}/(\Delta y)^2$. Incorporating the Newman boundary conditions at $i=0$, the Dirichlet boundary conditions at $i=M$ and the initial conditions, we have the following schemes:

Heat Numerical Model:

$$\begin{aligned}&-r^\theta\theta_{i-1}^{N+1}+(1+2r^\theta)\theta_i^{N+1}-r^\theta\theta_{i+1}^{N+1}=\theta_i^N,\ 0\le i\le M-1;\\ &\theta_{-1}^N=\theta_1^N\ and\ \theta_M^N=1\ for\ all\ N\ge 0;\ \theta_i^0=\theta(y_i,0)\ for\ all\ 0\le i\le M.\end{aligned} \tag{18}$$

Concentration Numerical Model:

$$\begin{aligned}&-r^f f_{i-1}^{N+1}+(1+2r^f)f_i^{N+1}-r^f f_{i+1}^{N+1}=\frac{\gamma}{4}r^f\left(f_{i+1}^N-f_{i-1}^N\right)^2+\lambda e^{nf_i^N},\ for\ 0\le i\le M-1;\\ &f_{-1}^N=f_1^N\ and\ f_M^N=1\ for\ all\ N\ge 0;\ f_i^0=f(y_i,0)\ for\ all\ 0\le i\le M.\end{aligned} \tag{19}$$

Velocity Numerical Model:

$$\begin{aligned}-r^w w_{i-1}^{N+1} + (1+2r^w) w_i^{N+1} - r^w w_i^{N+1} &= w_i^N + \frac{\alpha}{4} r^w (f_{i+1}^{N+1} - f_{i-1}^{N+1})(w_{i+1}^N - w_{i-1}^N) \\ &+ (G_c f_i^{N+1} + G_T \theta_i^{N+1} + K)\Delta t, \quad 0 \le i \le M-1, \\ w_{-1}^N = w_1^N \ \textit{for all} \ N \ge 0;\ w_i^0 &= w(y_i, 0) \ \textit{for all} \ 0 \le i \le M.\end{aligned} \tag{20}$$

Notice that equation (18) solves for the temperature independently, and the same can be said for the concentration in equation (19). Hence, all the temperature and concentration terms appearing in the velocity scheme (20), are already known and used to compute the velocity - this is why the proposed scheme is called sequential method. This completes the numerical formulation.

4. Numerical Results and Discussion

In this section, numerical results are presented to compare the proposed mathematical and numerical models. The convergence study is presented, the accuracy of the numerical method is then verified comparing with Matlab solver results. Time evolution of the flow fields are studied and finally, the effects of the flow parameters on the flow fields are presented. The numerical scheme presented in the previous section is implemented in an in-house C++ code developed by the author. Except otherwise stated, the following data is used for the computations:

$$\begin{aligned}&G_c = 0.1,\ G_T = 0.1,\ S_c = 0.6,\ \alpha = 0.1,\ \lambda = 0.5,\ n = 0.1,\ m = 0.1,\ K = 1, \\ &P_r = 0.72,\ \Delta t = 0.005,\end{aligned}$$

and the total duration of simulation is T = 60 seconds. We choose the Schmidt number to correspond to some chemical substances, namely hydrogen (0.22), water vapor (0.62), ammonia (0.78) and propyl (2.62), see [2, 21]. The other parameters are taken from previous studies such as [2, 21].

4.1. Convergence Analysis of the Scheme

In this subsection an experimental order of convergence (EOC) for the proposed numerical scheme is presented. The goal is to show that certainly the numerical results converge. A reference solution obtained from a simulation on a grid with 4096 cells or 4097 grid points is considered. The numerical scheme is then run for a sequence of grids with $M = 2^k,\ k = 2,3,4,\ldots,11$ grid points.

The error is considered in 2-norm defined as:

$$\left\| g_{ref}^N \right\|_{l_2} := \sqrt{h_{ref} \sum_{i=1}^{M_{ref}} g_{ref}^N [i]} \tag{21}$$

where $M_{ref} = 4097$ being the number of points in the reference grid, h_{ref} is the grid spacing and g_{ref}^N is a grid function - discrete function. The experimental order of convergence (EOC) is computed as:

$$EOC := \frac{\log_{10}\left(\dfrac{\left\| u_{ref}^N - u_h^N \right\|_{l_2}}{\left\| u_{ref}^N - u_{h/2}^N \right\|_{l_2}} \right)}{\log_{10} 2} \tag{22}$$

where u_{ref}^N , u_h^N and $u_{h/2}^N$ are the approximate solutions obtained using grid spacing, and h_{ref}, h and $h/2$ respectively, [26]. Observe that the coarse grids have less number of grid points than the fine (reference) mesh, hence we interpolate linearly to obtain the approximate solutions at intermediate points on the coarse grid as follows. Let u_l and u_r be the approximate solutions at grid points y_l and y_r respectively, and let $y \in [y_l, y_r]$, then we approximate the solution at y using the formula:

$$u(y) \approx \frac{u_l y_r - u_r y_l + (u_r - u_l) y}{y_r - y_l}, \quad \text{for all } y \in [y_l, y_r]. \tag{23}$$

Table 1 shows the results of the simulations on the various grids including the 2-norm error and the experimental order of convergence for each solution variable. The time step is chosen as 0.0001 and terminate after 0.001 seconds. It can be seen that as the grid is being refined, the errors for all variables are decreasing, hence the scheme converges. Also, it can be observed that the order of convergence for the temperature is approximately two as expected, this is due the temperature model being linear with constant coefficient, hence the theoretical order of convergence is highly recovered. It can also be noticed from the table that the order of convergence for the velocity and concentration is good, though not two. This is due to the fact that the nonlinear velocity and concentration models they have been linearized. Overall, the table shows that the convergence of the proposed scheme is guaranteed.

Table 1. Experimental order of convergence, $Error_w$, $Error_f$ and $Error_\theta$ are the errors in w, f and θ respectively, while EOC_w, EOC_f and EOC_θ are their respective numerical orders of accuracy.

M -1	$Error_w$	EOC_w	$Error_f$	EOC_f	$Error_\theta$	EOC_θ
4	0.00131136	-	0.1812	-	0.192327	-
8	0.000402004	1.70578	0.0713787	1.34402	0.0824526	1.22192
16	0.000153622	1.38783	0.0178135	2.00252	0.0224425	1.87733
32	7.22053e-05	1.08921	0.00436927	2.02751	0.00546173	2.0388
64	3.60866e-05	1.00064	0.00107911	2.01755	0.0013584	2.00744
128	1.7966e-05	1.00619	0.000265853	2.02114	0.000339055	2.00232
256	8.76012e-06	1.03625	6.44961e-05	2.04334	8.463e-05	2.00228
512	4.10541e-06	1.09342	1.51911e-05	2.08599	2.10491e-05	2.00741
1024	1.76335e-06	1.2192	3.43109e-06	2.14649	5.15294e-06	2.03029
2048	5.8845e-07	1.58333	7.5812e-07	2.17817	1.16783e-06	2.14156

4.2. Verification of the Numerical Scheme against Matlab Solver

In this section, the numerical scheme is verified by comparing its numerical results with those obtained from a Matlab subroutine, the ***pdepe*** solver. To do this, the results of each scheme for the spatial distribution of velocity, concentration and temperature are shown. Figure 2(a) shows the velocity distributions computed with the proposed scheme at the different times indicated, while 2(b) shows those computed using the Matlab solver. It can be seen that the results of the proposed method agree with those of the Matlab solver. The same agreement is also observed for the concentration distributions, see figures 3(a) and 3(b), and for the temperature distributions, see figures 4(a) and 4(b).

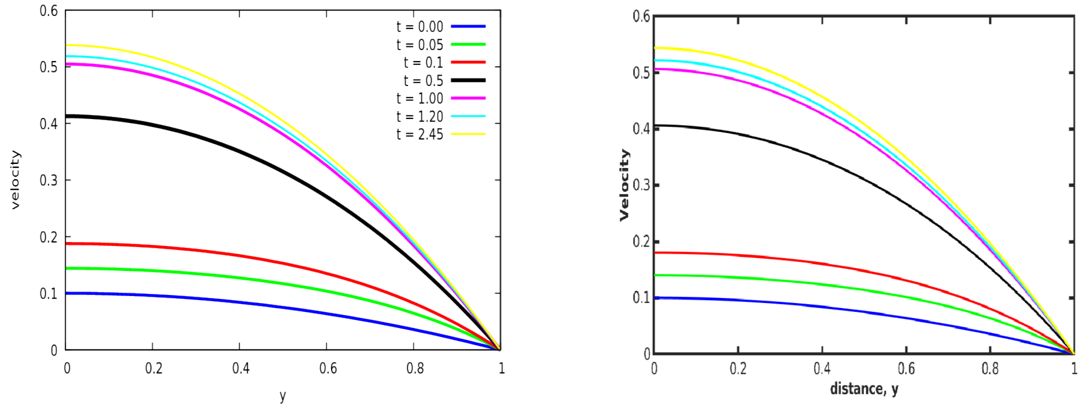

(a) Proposed scheme (b) Matlab PDE solver

Fig. 2. Comparison of the proposed scheme with Matlab PDE solver for velocity distribution at different times

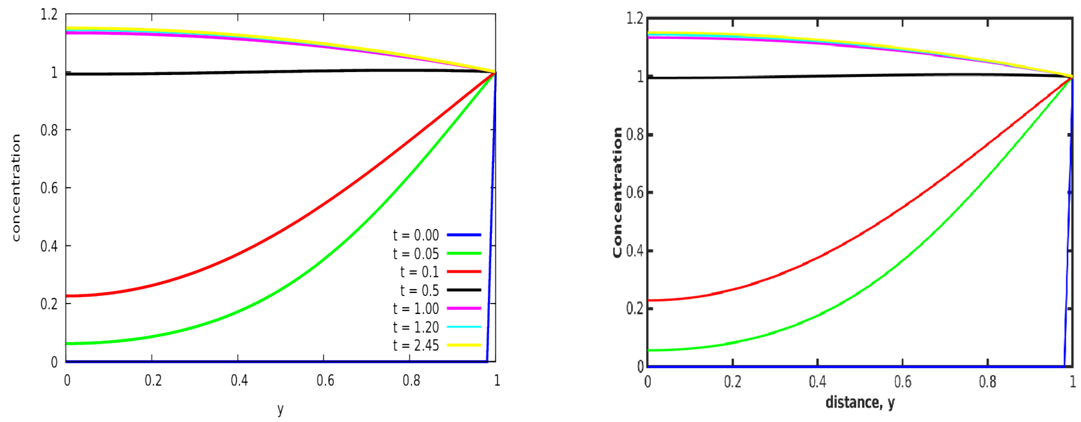

(a) Proposed scheme (b) Matlab PDE solver

Fig. 3. Comparison of the proposed scheme with Matlab PDE solver for concentration distribution at different times

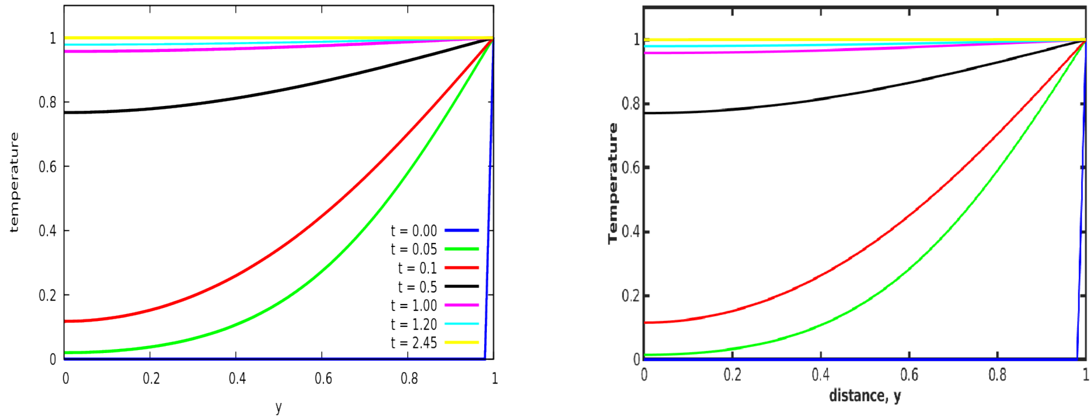

(a) Proposed scheme (b) Matlab PDE solver

Fig. 4. Comparison of the proposed scheme with Matlab PDE solver for temperature distribution at different times

4.3. Spatial Distribution of Flow Fields

Figures 5(a), 5(b) and 5(c) show the spatial distribution of the velocity, concentration and temperature, respectively, at different time instants. First, one can see that the specified boundary conditions in (14) are correctly reproduced for all the three flow fields. As observed in [2], the injection of pollutant acts as momentum source, hence should lead to increase in both the velocity and concentration profile. Moreover, the heating of the plate transfers heat into the fluid which also acts as momentum source, hence the velocity is expected to increase with time. This is clearly the case for the velocity profile in figure 5(a). Both the velocity and concentration increased and settled at their steady state conditions after some time. This is in agreement with the observation made in [2].

It can also be seen that the temperature profiles in figure 5(c) reproduced the correct physical phenomenon as one would expect, namely at initial time the fluid had zero temperature but the wall is being heated at a constant temperature, hence as time increases, the fluid temperature will attain a maximum temperature equal to the constant temperature of the wall. This is exactly reproduced in the numerical results in figure 5(c).

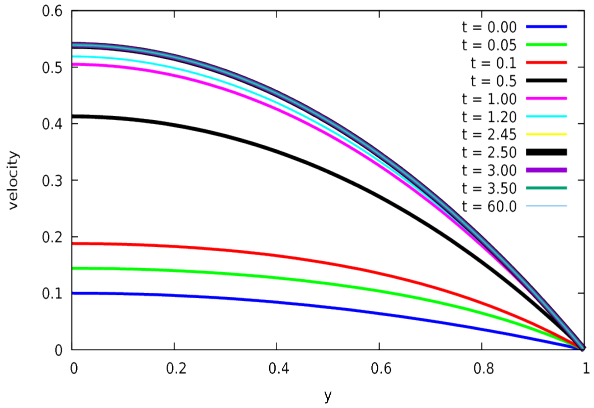

(a) Variation of velocity

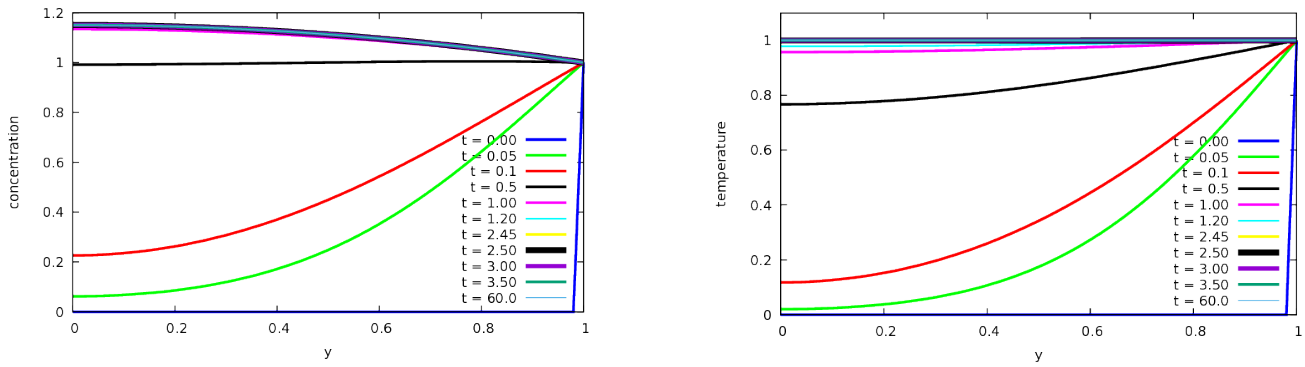

(b) Variation of concentration (c) Variation of temperature

Fig. 5. Spatial distribution of flow fields

4.4. Influence of the Flow Parameters on the Flow Fields

In this section the results for the influence of the flow parameters on the flow fields are presented and discussed. Except otherwise stated, the results are outputted at time 1.05 seconds.

4.4.1. Variations with Solutal Grashof Number, G_c

The solutal Grashof number, G_c acts as a source in the momentum equation but does not appear in the concentration and temperature equations hence its increase is expected to increase the velocity but have no influence on the concentration nor the temperature. The achieved results in figures 6(a) to 6(c) reproduced these facts exactly. This is in accordance with the results of [2, 20].

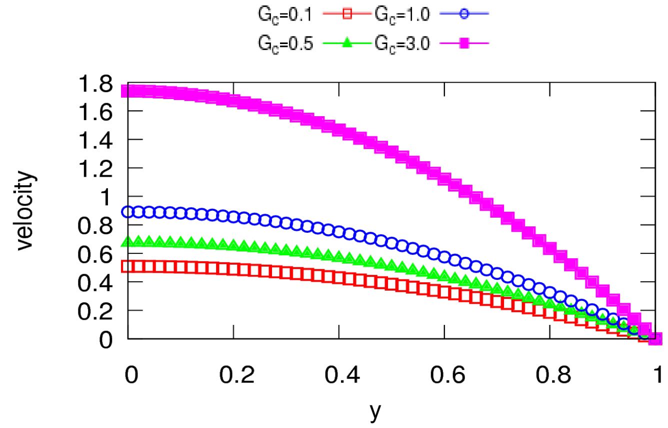

(a) Variation of velocity with G_c

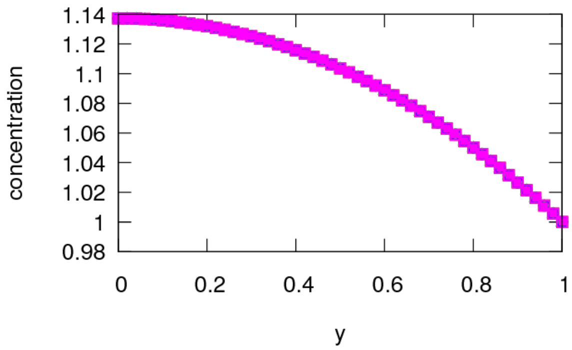

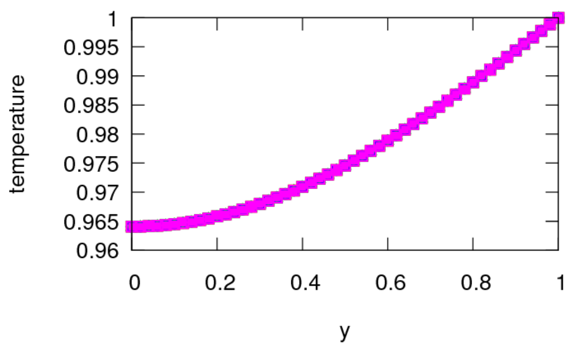

(b) Variation of concentration with G_c (c) Variation of temperature with G_c

Fig. 6. Effect of Solutal Grashof's number G_c

4.4.2. Variations with Thermal Grashof Number, G_T

The thermal Grashof number, G_T also does not appear in either the concentration or temperature equations, hence should have no influence on the concentration and temperature fields, but should increase the velocity. These facts are accurately reproduced in figures 7(a) - 7(c).

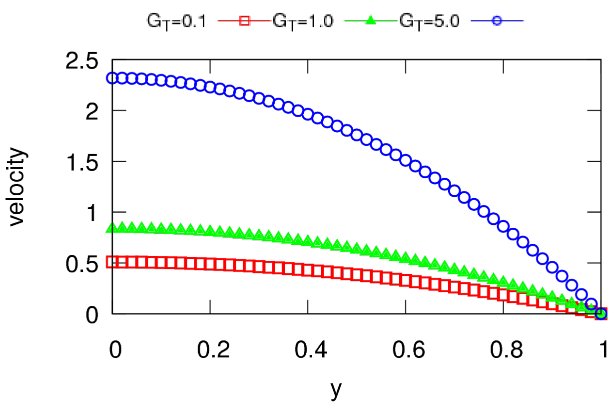

(a) Variation of velocity with G_T

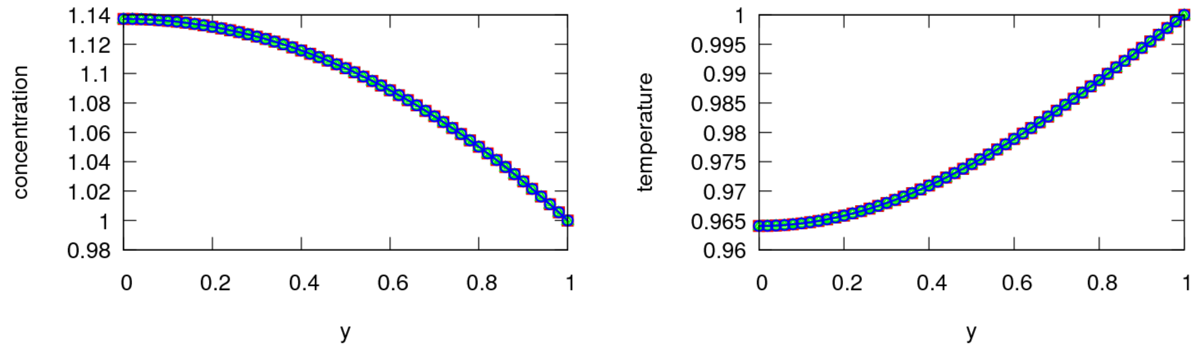

(b) Variation of concentration with G_T (c) Variation of temperature with G_T

Fig. 7. Effect of Thermal Grashof's number G_T

4.4.3. Variations with Schmidt Number, S_c

The depicted results in figure 8(a) - show that increase in the Schmidt number increases the concentration. This is due to the fact that an increased Schmidt number is associated with reducing the dispersion (or diffusion) of the pollutant (see equation (10)), hence the concentration increases. On the other hand, an increase in the Schmidt number leads to no significant change in the velocity - see figure 8(b). This is because a concentration increase, leads to increase in both the source term and the fluid concentration-dependent viscosity in the momentum equation. These are two opposing factors (increased source increases velocity while the increased viscosity reduces velocity) whose resultant effect has no significant effect on the velocity. The temperature is not affected by this parameter.

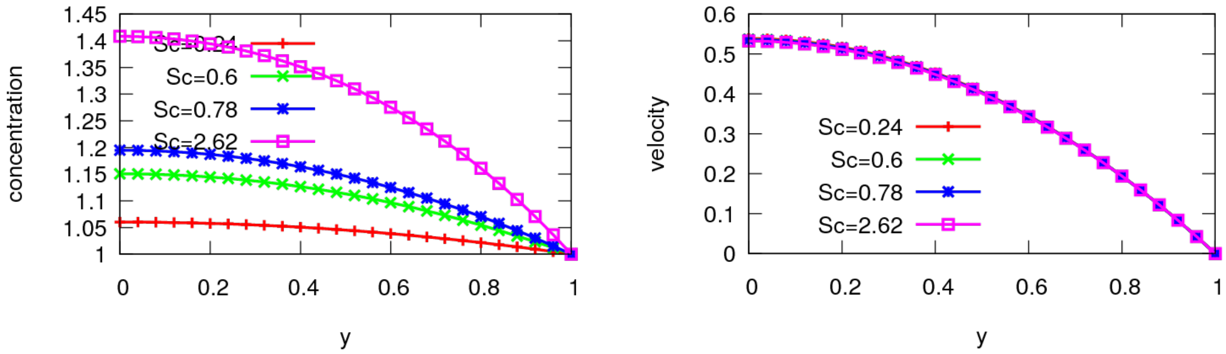

(a) Variation of concentration with S_c (b) Variation of velocity with S_c

Fig. 8. Effect of Schmidt Grashof's number S_c

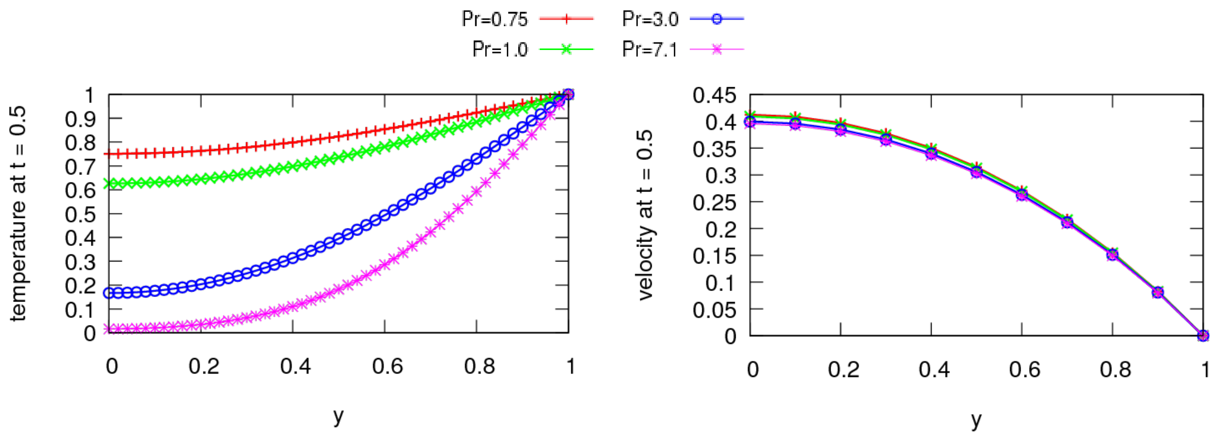

(a) Variation of temprature with P_r (b) Variation of velocity with P_r

Fig. 9. Effect of Prandtl number P_r

4.4.4. Variations with Prandtl Number, P_r

The obtained results show that increase in the Prandtl number leads to a decrease in the temperature - see figure 9(a) -

which agrees with the result in [27]. Since the temperature is decreased with increased Prandtl number, it means that the temperature source term in the momentum equation should also decrease, hence decreasing the velocity. This is shown in figure 9(b) in which the velocity is slightly decreased. The Prandtl number has no effect on the concentration, this is expected since it does not appear in the concentration model.

4.4.5. Variations with α

Our results show that increased α reduced the velocity, see figure 10(a). This is expected since increasing α means increasing the fluid viscosity, hence decreasing velocity. The parameter has no effect on neither concentration nor temperature.

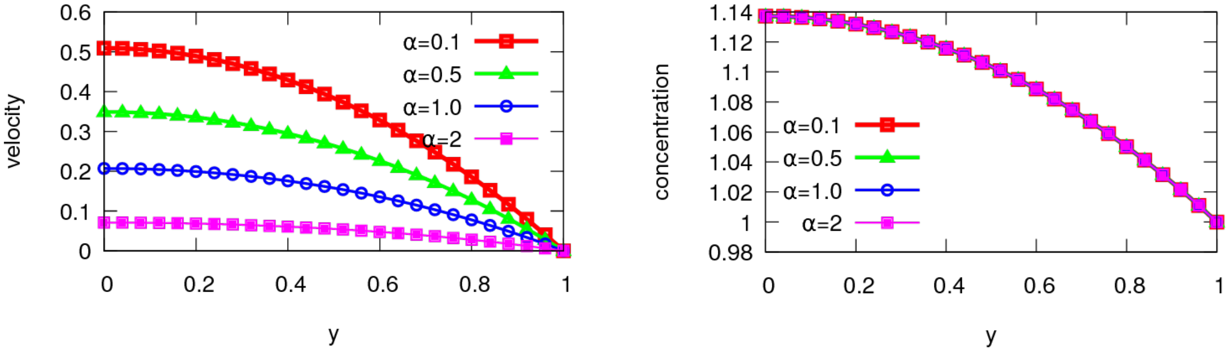

(a) Variation of velocity with α (b) Variation of concentration with α

Fig. 10. Effect of velocity and concentration with α

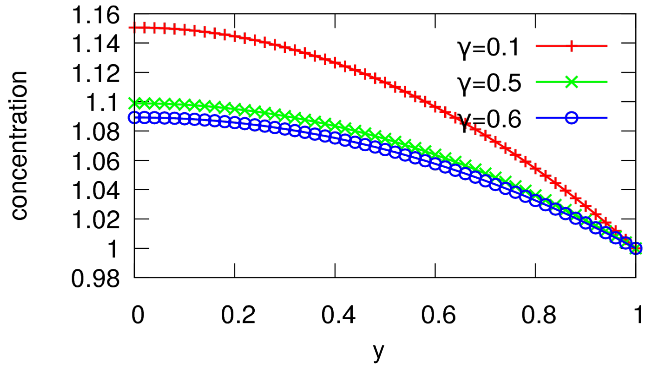

(a) Variation of concentration with γ

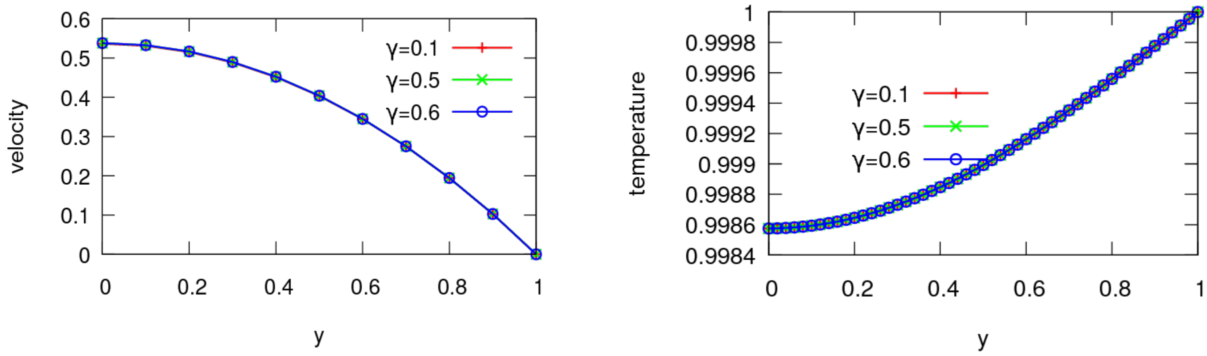

(b) Variation of velocity with γ (c) Variation of temperature with γ

Fig. 11. Effect of γ

4.4.6. Variations with γ

Figures 11(a)-11(c) are the results outputted after 2 seconds for different values of γ. Figure 11(a) shows that the concentration decreases with increasing γ. This is the expected result since increasing γ means increasing the pollutant dispersion (diffusion), hence the concentration decreases. On the other hand, an increase in γ leads to no significant change in the velocity (see figure 11(b)) nor the temperature - figure 11(c).

4.4.7. Variations with λ

Figures 12(a) to 12(b) show the effects of the parameter, λ on the flow fields. From our modelling assumptions, increasing λ means increasing the pollutant injection into the fluid, hence should increase the concentration. This is exactly what is observed in figure 12(a). Figure 12(b) shows that the velocity is slightly decreasing with increased λ. This is also due to the fact that concentration is increased leading to increased momentum source which is surpassed by the velocity reduction arising from increased fluid viscosity, hence the marginal decrease of velocity observed in figure 12(b). This parameter has no effect on the temperature.

4.4.8. Variations with n

This parameter, n has to do with the pollutant injection, hence its increase should increase the concentration, and this is clearly observed in figure 13(a). However, no significant effect is observed on the velocity - figure 13(b).

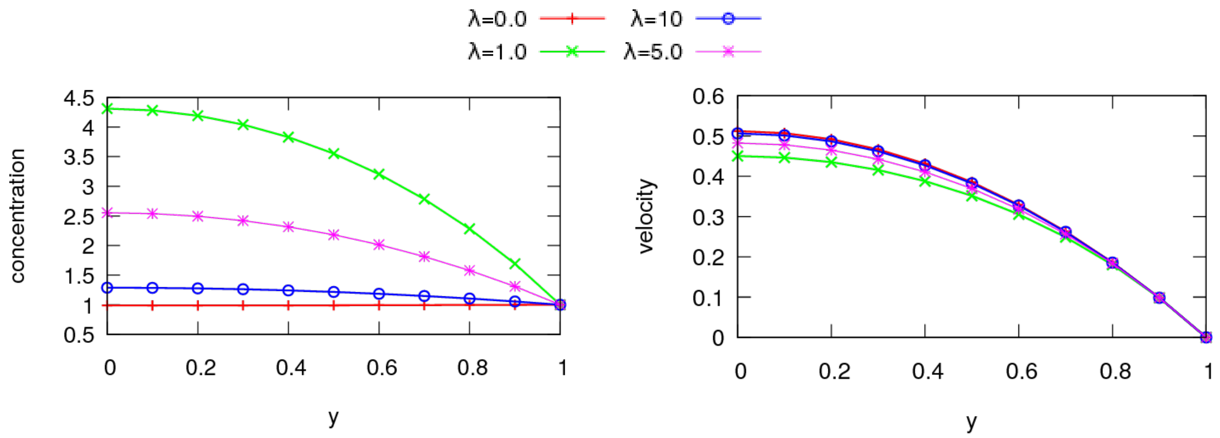

(a) Variation of concentration with λ (b) Variation of velocity with λ

Fig. 12. Effect of λ

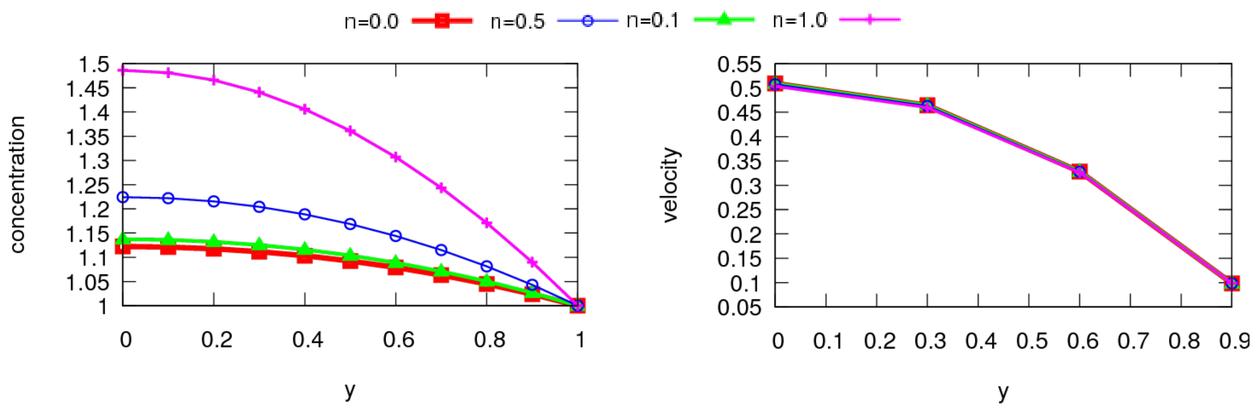

(a) Variation of concentration with n (b) Variation of velocity with n

Fig. 13. Effect of n

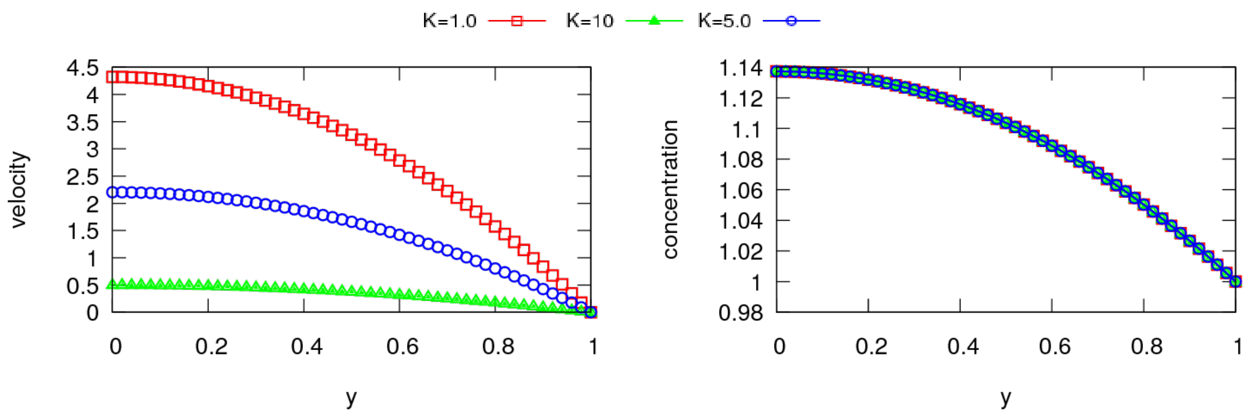

(a) Variation of velocity with K (b) Variation of concentration with K

Fig. 14. Effect of K

4.4.9. Variations with K

As one would expect, an increase in pressure gradient should increase the fluid velocity. Figure 14(a) shows the effect of the pressure gradient parameter, K on the fluid velocity. We can see that, indeed, the velocity increases as this parameter is increased. The parameter does not affect the concentration and temperature as expected, see figure 14(b).

5. Conclusion

In this paper a sequential implicit finite difference formulation to study the flow of fluid with pollutant dispersion and heat transfer is presented and analyzed. It is observed that a change in the pollutant concentration only leads to very small change in the fluid velocity due to the opposing effects of increased source term and increased viscosity. Also, decreasing the temperature - by increasing the Prandtl number - resulted to only small decrease in the fluid velocity. These are in agreement with those of previous studies. The presented numerical experiments and convergence analysis also show that the computed results are in good agreement with well-established solvers, and their errors vanish as the grid is refined. It is therefore, concluded that the proposed sequential method computes physically correct results and is convergent.

Acknowledgments

The author is grateful to God for all things. He is indebted to the Petroleum Technology Development Fund (PTDF), Nigeria for funding his PhD at the University of Warwick, United Kingdom during 2012-2016. A big thanks to the Mathematical and Scientific Computing Solutions (MSCS) Limited (Nigeria) for providing the computing resources. Finally, the author is grateful to the reviewers for their valuable suggestions that greatly improved the work.

Conflict of Interest

The author declared no potential conflicts of interest with respect to the research, authorship and publication of this article.

Funding

The author received no financial support for the research, authorship and publication of this article.

References

[1] G.V. Ramana Reddy, N. Bhaskar Reddy, R.S.R. Gorla, Radiation and chemical reaction effects on mhd flow along a moving vertical porous plate. *International Journal of Applied Mechanics and Engineering*, 21(1), 2016, 157–168.

[2] T. Chinyoka, O.D., Makinde, Analysis of nonlinear dispersion of a pollutant ejected by an external source into a channel flow. *Mathematical Problems in Engineering*, 2010, Article ID 827363, 17 p.

[3] O.D. Makinde, T. Chinyoka, Numerical investigation of transient heat transfers to hydromagnetic channel flow with radiative heat and convective cooling. *Communications in Nonlinear Science and Numerical Simulation*, 15(12), 2010, 3919–3930.

[4] J.C. Umavathi, M.A. Sheremet, S. Mohiuddin, Combined effect of variable viscosity and thermal conductivity on mixed convection flow of a viscous fluid in a vertical channel in the presence of first order chemical reaction. *European Journal of Mechanics-B/Fluids*, 58, 2016, 98–108.

[5] J.C. Umavathi, J.P. Kumar, M.A. Sheremet, Heat and mass transfer in a vertical double passage channel filled with electrically conducting fluid. *Physica A: Statistical Mechanics and its Applications*, 465, 2017, 195–216.

[6] R. Bhargava, R. Sharma, O.A. Beg, Oscillatory chemically-reacting mhd free convection heat and mass transfer in a porous medium with soret and dufour effects - finite element modelling. *International Journal of Applied Mathematics and Mechanics*, 5(6), 2009, 15–37.

[7] P. Mebine, Radiation effects on mhd couette flow with heat transfer between two parallel plates. *Journal of Pure Applied Mathematics*, 3(2), 2007, 191–202.

[8] C. Israel-Cookey, E. Amos, C. Nwaigwe, Mhd oscillatory couette flow of a radiating viscous fluid in a porous medium with periodic wall temperature. *American Journal of Scientific and Industrial Research*, 1(2), 2010, 326–331.

[9] C. Israel-Cookey, C. Nwaigwe, Unsteady mhd flow of a radiating fluid over a moving heated porous plate with time-dependent suction. *American Journal of Scientific and Industrial Research*, 1(1), 2010, 88–95.

[10] C. Nwaigwe, Mathematical modelling of ground temperature with suction velocity and radiation. *American Journal of Scientific and Industrial Research*, 1(2), 2010, 238–241.

[11] R.K. Selvi, R. Muthuraj, Mhd oscillatory flow of a jeffrey fluid in a vertical porous channel with viscous dissipation. *Ain Shams Engineering Journal*, 9(4), 2018, 2503-2516.

[12] T. Hayat, M. Mustafa, S. Asghar, Unsteady flow with heat and mass transfer of third grade fluid over a stretching surface in the presence of chemical reaction. *Nonlinear Analysis, Real World Application*, 11, 2010, 3186– 3197.

[13] K. Kavita, P.K., Ramakrishna, K.B., Aruna, Influence of heat transfer on mhd oscillatory flow of jeffrey fluid in a channel. *Advanced Applied Scientific Research*, 3, 2012, 2312–2325.

[14] R. Muthuraj, S. Srinivas, A.K. Shukla, T.R. Ramamohan, Effects of thermal-diffusion, diffusion-thermo and space porosity on mhd mixed convection flow of micropolar fluid in a vertical channel with viscous dissipation. *Asian Research*, 43, 2014, 561–578.
[15] J.K. Singh, N. Joshi, S.G. Begum, Unsteady hydromagnetic heat and mass transfer natural convection flow past an exponentially accelerated vertical plate with hall current and rotation in the presence of thermal and mass diffusions. *Frontiers in Heat and Mass Transfer*, 7(24), 2016, 1-12.
[16] J.C. Umavathi, M.A. Sheremet, Mixed convection flow of an electrically conducting fluid in a vertical channel using robin boundary conditions with heat source/sink. *European Journal of Mechanics-B/Fluids*, 55, 2016, 132–145.
[17] S.M. Ibrahim, G. Lorenzini, P.V. Kumar, C.S.K. Raju, Influence of chemical reaction and heat source on dissipative mhd mixed convection flow of a casson nanofluid over a nonlinear permeable stretching sheet. *International Journal of Heat and Mass Transfer*, 111, 2017, 346–355.
[18] L.N. Moresi, V.S. Solomatov, Numerical investigation of 2d convection with extremely large viscosity variations. *Physics of Fluids*, 7(9), 1995, 2154–2162.
[19] T. Chinyoka, O.D. Makinde, Computational dynamics of unsteady flow of a variable viscosity reactive fluid in a porous pipe. *Mechanics Research Communications*, 37(3), 2010, 347–353.
[20] J.C. Umavathi, M.A. Sheremet, Influence of temperature dependent conductivity of a nanofluid in a vertical rectangular duct. *International Journal of Non-Linear Mechanics*, 78, 2016, 17–28.
[21] O.D. Makinde, T. Chinyoka, Transient analysis of pollutant dispersion in a cylindrical pipe with a nonlinear waste discharge concentration. *Computers and Mathematics with Applications*, 60, 2010, 642–652.
[22] R.A Van Gorder, K. Makowski, K. Mallory, K. Vajravelu, Self-similar solutions for the nonlinear dispersion of a chemical pollutant into a river flow. *Journal of Mathematical Chemistry*, 53(7), 2015, 1523–1536.
[23] O.D. Makinde, R.J. Moitsheki, B.A. Tau, Similarity reductions of equations for river pollution. *Applied Mathematics and Computation*, 188(2), 2007, 1267–1273.
[24] R.J. Moitsheki, O.D. Makinde, Symmetry reductions and solutions for pollutant diffusion in a cylindrical system. *Nonlinear Analysis: Real World Applications*, 10(6), 2009, 3420–3427.
[25] O.D. Makinde, P. Olanrewaju, W.M. Charles, Unsteady convection with chemical reaction and radiative heat transfer past a flat porous plate moving through a binary mixture. *Journal of African Mathematical Union*, 22, 2011, 65–78.
[26] C. Nwaigwe, Coupling Methods for 2D/1D Shallow Water Flow Models for Flood Simulations. PhD thesis, University of Warwick, United Kingdom, 2016.
[27] T. Chinyoka, O.D. Makinde, Analysis of transient generalized couette flow of a reactive variable viscosity third-grade liquid with asymmetric convective cooling. *Mathematical and Computer Modelling*, 54(1-2), 2011, 160–174.